

# Matter Effects on Neutrino Oscillations in Long Baseline Experiments

Irina Mocioiu<sup>1(a)</sup> and Robert Shrock<sup>2(a,b)</sup>

(a) C.N. Yang Institute for Theoretical Physics  
 State University of New York  
 Stony Brook, NY 11794-3840  
 (b) Physics Department  
 Brookhaven National Laboratory  
 Upton, NY 11973

## Abstract

We calculate matter effects on neutrino oscillations relevant for long baseline experiments. In particular, we compare the results obtained with constant density along the neutrino path versus results obtained by incorporating the actual density profiles in the Earth. We study the dependence of the oscillation signal on both  $E/\Delta m_{atm}^2$  and on the angles in the leptonic mixing matrix. We also comment on the influence of  $\Delta m_{sol}^2$  on the oscillations. The results show quantitatively how, as a function of these input parameters, matter effects can cause significant ( 25 %) changes in the oscillation probabilities. An important conclusion is that matter effects can be useful in amplifying certain neutrino oscillation signals and helping one to obtain measurements of mixing parameters and the magnitude and sign of  $\Delta m_{atm}^2$ .

---

<sup>1</sup>email: mocioiu@insti.physics.sunysb.edu

<sup>2</sup>email: shrock@insti.physics.sunysb.edu

# 1 Introduction

In a modern theoretical context, one generally expects nonzero neutrino masses and associated lepton mixing. Experimentally, there has been accumulating evidence for such masses and mixing. All solar neutrino experiments (Homestake, Kamiokande, SuperKamiokande, SAGE, and GALLEX) show a significant deficit in the neutrino fluxes coming from the Sun [1]. This deficit can be explained by oscillations of the  $\nu_e$ 's into other weak eigenstate(s), with  $\Delta m_{sol}^2$  of the order  $10^{-5}$  eV $^2$  for solutions involving the Mikheev-Smirnov-Wolfenstein (MSW) resonant matter oscillations [2, 3] or of the order of  $10^{-10}$  eV $^2$  for vacuum oscillations. Accounting for the data with vacuum oscillations (VO) requires almost maximal mixing. The MSW solutions include one for small mixing angle (SMA) and one with essentially maximal mixing (LMA).

Another piece of evidence for neutrino oscillations is the atmospheric neutrino anomaly, observed by Kamiokande [4], IMB [5], SuperKamiokande [6] with the highest statistics, and by Soudan [7] and MACRO [8]. This data can be fit by the inference of  $\nu_\mu \rightarrow \nu_x$  oscillations with  $\Delta m_{atm}^2 \sim 3.5 \times 10^{-3}$  eV $^2$  and maximal mixing  $\sin^2 2\theta_{atm} = 1$  [6]. The identification  $\nu_x = \nu_\tau$  is preferred over  $\nu_x = \nu_{sterile}$  at about the  $2.5\sigma$  level [9], and the identification  $\nu_x = \nu_e$  is excluded by both the Superkamiokande data and the Chooz experiment [10, 11].

In addition, the LSND experiment has reported observing  $\bar{\nu}_\mu \rightarrow \bar{\nu}_e$  and  $\nu_\mu \rightarrow \nu_e$  oscillations with  $\Delta m_{LSND}^2 \sim 0.1 - 1$  eV $^2$  and a range of possible mixing angles, depending on  $\Delta m_{LSND}^2$  [12]. This result is not confirmed, but also not completely ruled out, by a similar experiment, KARMEN [13].

There are currently intense efforts to confirm and extend the evidence for neutrino oscillations in all of the various sectors – solar, atmospheric, and accelerator. Some of these experiments are running; these include the Sudbury Neutrino Observatory, SNO, and the K2K long baseline experiment between KEK and Kamioka. Others are in development and testing phases, such as BOONE, MINOS, the CERN - Gran Sasso program, KAMLAND, and Borexino [14]. Among the long baseline neutrino oscillation experiments, the approximate distances are  $L \simeq 250$  km for K2K, 730 km for both MINOS, from Fermilab to Soudan and the proposed CERN-Gran Sasso experiments. The sensitivity of these experiments is projected to reach down roughly to the level  $\Delta m^2 \sim 10^{-3}$  eV $^2$ . There is strong motivation for another generation of experiments with even higher sensitivity that can confirm the  $\nu_\mu \rightarrow \nu_\tau$  transition with the values of  $\Delta m_{atm}^2$  and  $\sin^2 2\theta_{atm}$  reported so far and carry out further measurements of various neutrino oscillation channels.

Recently, there has been considerable interest in the idea of a muon storage ring that would serve as a “neutrino factory”, i.e., a source of quite high intensity, flavor-pure neutrino and antineutrino beams:  $\nu_\mu + \bar{\nu}_e$  ( $\bar{\nu}_\mu + \nu_e$ ) from stored  $\mu^-$ 's ( $\mu^+$ 's) respectively [15]-[20]. Given the very high intensities anticipated to be of order  $10^{20}$  and perhaps even  $10^{21}$  muon decays per year in various preliminary studies, one can envision neutrino oscillation experiments with quite long baselines of order several thousand km, with commensurate sensitivity to various neutrino oscillation channels.

One of the appeals of the muon storage ring/neutrino factory is that one can measure several different neutrino oscillation transitions, using both the  $\nu_\mu$  ( $\bar{\nu}_\mu$ ) and  $\bar{\nu}_e$  ( $\nu_e$ ) from a

$\mu^-$  ( $\mu^+$ ) beam. In this paragraph we assume a  $\mu^-$  beam for definiteness (figures below are shown for neutrinos from both stored  $\mu^+$  and  $\mu^-$  beams). In addition to a high-statistics measurement of  $\nu_\mu \rightarrow \nu_\mu$ , as a disappearance test for the  $\nu_\mu \rightarrow \nu_\tau$  oscillation, one has also various other channels. Among these are  $\bar{\nu}_e \rightarrow \bar{\nu}_\mu$ , for which the signal is a “wrong-sign muon”,  $\mu^+$ , and  $\bar{\nu}_e \rightarrow \bar{\nu}_\tau$ , which, in about 18 % of its decays, would also yield a wrong-sign muon. The measurement of the muon charge would be possible with either a magnetized iron detector or a combination of a massive water Čerenkov detector followed by a muon spectrometer. With sufficient detector capabilities, one could also search for  $\tau$  appearance, as is envisioned by the ICANOE and OPERA experiments at Gran Sasso [21, 22], although this requires neutrino energies  $E_\nu \gtrsim 20$  GeV to avoid kinematic suppression of  $\tau$  production.

An important effect that must be taken into account in such experiments concerns the matter-induced oscillations which neutrinos undergo along their flight path through the Earth from the source to the detector. Given the typical density of the earth, matter effects are important for the neutrino energy range  $E \sim O(10)$  GeV and  $\Delta m_{atm}^2 \sim 3 \times 10^{-3}$  eV<sup>2</sup> values relevant for the long baseline experiments, in particular, for the oscillation channels involving  $\nu_e$ , as we shall show below. Matter effects can also be important for the neutrino energy range  $E \sim O(10)$  MeV and  $\Delta m^2 \sim 10^{-5}$  eV<sup>2</sup> involved in MSW solutions to the solar neutrino problem. After the initial discussion of matter-induced resonant neutrino oscillations in [2], an early study of these effects including three generations was carried out in [23]. The sensitivity of an atmospheric neutrino experiment to small  $\Delta m^2$  due to the long baselines and the necessity of taking into account matter effects was discussed e.g., in [24]. After Ref. [3], many analyses were performed in the 1980’s of the effects of resonant neutrino oscillations on the solar neutrino flux, and matter effects in the Earth were studied, e.g., [25] and [26], which also discussed the effect on atmospheric neutrinos (see also the review [27]). Recent papers on matter effects relevant to atmospheric neutrinos include [28, 29]. An early study of matter effects on long baseline neutrino oscillation experiments was carried out in [30]. More recent analyses relevant to neutrino factories include [15, 16], [31]-[35].

In this paper we shall present calculations of the matter effect for parameters relevant to possible long baseline neutrino experiments envisioned for the muon storage ring/neutrino factory. In particular, we compare the results obtained with constant density along the neutrino path versus results obtained by incorporating the actual density profiles. We study the dependence of the oscillation signal on both  $E/\Delta m_{atm}^2$  and on the angles in the leptonic mixing matrix. We also comment on the influence of  $\Delta m_{sol}^2$  and CP violation on the oscillations. Some of our results were presented in Ref. [36]. Additional recent studies include [37]-[40].

In a hypothetical world in which there were only two neutrinos,  $\nu_\mu$  and  $\nu_\tau$ , the  $\nu_\mu \rightarrow \nu_\tau$  oscillations in matter would be the same as in vacuum, since both have the same forward scattering amplitude, via  $Z$  exchange, with matter. However, in the realistic case of three generations, because of the indirect involvement of  $\nu_e$  due to a nonzero  $U_{13}$ , and because of the fact that  $\nu_e$  has a different forward scattering amplitude off of electrons, involving both  $Z$  and  $W$  exchange, there will be a matter-induced oscillation effect on  $\nu_\mu \rightarrow \nu_\tau$  (as well as other channels).

We consider the usual three flavors of active neutrinos, with no light sterile (=electroweak-

singlet) neutrinos. This is sufficient to describe the solar and atmospheric neutrino deficit. If one were also to include the LSND experiment, then, to obtain a reasonable fit, one would be led to include light electroweak-singlet neutrinos. Since the LSND experiment has not so far been confirmed, we shall, while not prejudging the outcome of the BOONE experiment, not include this in our fit. We calculate oscillation probabilities in the full  $3 \times 3$  mixing case and we study when  $\Delta m_{sol}^2$  can be relevant. In most cases there is only one mass scale relevant for long baseline neutrino oscillations,  $\Delta m_{atm}^2 \sim \text{few} \times 10^{-3} \text{ eV}^2$  and we work with the hierarchy

$$\Delta m_{21}^2 = \Delta m_{sol}^2 \ll \Delta m_{31}^2 \approx \Delta m_{32}^2 = \Delta m_{atm}^2 \quad (1)$$

In our work we take into account the actual profile of the Earth, as given by geophysical seismic data [41] and compare the results with those calculated using the approximation of average density along the path of the neutrino. Further, when only one mass squared difference is relevant, we present the oscillation probabilities as functions of  $E/\Delta m^2$ , where here and below,  $E = E_\nu$ . This way of presenting the results is useful since, for a given  $L$  value, it shows the matter effect for a wide range of  $E$  and  $\Delta m^2$  and hence can serve as an input in the choice of optimal beam energy (along with other considerations such as the cross section dependence  $\sigma \sim E$  and the beam divergence  $\sim (LE)^{-2}$ , which, together, favor higher values of  $E$  to achieve a high event rate). We study how these oscillation probabilities vary with the different input parameters and discuss the influence of the matter effects on the sensitivity to each of these parameters.

## 2 Theoretical Framework

We first recall the form of the lepton mixing matrix. Let us denote the flavor vectors of  $SU(2) \times U(1)$  nonsinglet neutrinos as  $\nu = (\nu_e, \nu_\mu, \nu_\tau)$  and the vector of electroweak-singlet neutrinos as  $\chi = (\chi_1, \dots, \chi_{n_s})$ . The Dirac and Majorana neutrino mass terms can then be written compactly as

$$-\mathcal{L}_m = \frac{1}{2}(\bar{\nu}_L \ \bar{\chi}^c_L) \begin{pmatrix} M_L & M_D \\ (M_D)^T & M_R \end{pmatrix} \begin{pmatrix} \nu_R^c \\ \chi_R \end{pmatrix} + h.c. \quad (2)$$

where  $M_L$  is the  $3 \times 3$  left-handed Majorana mass matrix,  $M_R$  is a  $n_s \times n_s$  right-handed Majorana mass matrix, and  $M_D$  is the 3-row by  $n_s$ -column Dirac mass matrix. In general, all of these are complex, and  $(M_L)^T = M_L$ ,  $(M_R)^T = M_R$ . Without further theoretical input, the number  $n_s$  of electroweak singlet neutrinos is not determined. For example, in the minimal  $SU(5)$  grand unified theory (GUT),  $n_s = 0$ , while in  $SO(10)$ ,  $n_s = 3$ . Within this theoretical context, since the terms  $\chi_{jR}^T C \chi_{kR}$  are electroweak singlets, the associated coefficients, which comprise the elements of the matrix  $M_R$ , would not be expected to be related to the electroweak symmetry breaking scale, but instead, would be expected to be much larger, plausibly of order the GUT scale. Furthermore, the left-handed Majorana mass terms can only arise via operators of dimension at least 5, such as

$$\mathcal{O} = \frac{1}{M_X} \sum_{a,b} h_{a,b} (\epsilon_{ik} \epsilon_{jm} + \epsilon_{im} \epsilon_{jk}) [\mathcal{L}_{aL}^{Ti} C \mathcal{L}_{bL}^j] \phi^k \phi^m + h.c. \quad (3)$$

where  $\mathcal{L}_{La} = (\nu_{\ell_a}, \ell_a)_L^T$  is the left-handed,  $I = 1/2$ ,  $Y = -1$  lepton doublet with generation index  $a$  ( $a = 1, 2$ , or  $3$ ), where  $\ell_a = e, \mu, \tau$ , for  $a = 1, 2, 3$ ,  $M_X$  denotes a generic mass scale characterizing the origin of this term, and  $\phi$  is the standard model Higgs or  $H_u$  in the supersymmetric standard model. Because (3) is a nonrenormalizable operator, the success of the standard model as a renormalizable field theory then implies that  $M_X$  is much larger than the scale of electroweak symmetry breaking, and, within a GUT context,  $M_X$  would be of order the GUT scale, as with  $M_R$ . The terms arising from the vacuum expectation values of the Higgs doublets then make up the submatrix  $M_L$ . The resultant diagonalization of the matrix in eq. (2) then naturally leads to a set of 3 light masses for the three known neutrinos, generically of order  $m_\nu \sim m_D^2/M_R$ , and  $n_s$  very large masses generically of order  $M_R$ , for the electroweak singlet neutrinos. This seesaw mechanism is very appealing, since it can provide a plausible explanation for why the known neutrinos are so light [42]. Although the full leptonic mixing matrix is  $(3 + n_s) \times (3 + n_s)$  dimensional, the light and heavy neutrinos largely decouple from each other so that, to a high degree of accuracy, one can describe the linear combinations of the  $(3 + n_s)$  mass eigenstates that form  $(3 + n_s)$  weak eigenstates in a decoupled manner, using a simple  $3 \times 3$  matrix  $U$ , which, to high accuracy, is unitary, for the known neutrinos. This is determined by the diagonalization of the effective  $3 \times 3$  light neutrino mass matrix

$$M_\nu = -M_D M_R^{-1} M_D^T \quad (4)$$

and an  $n_s \times n_s$  matrix for the heavy neutrino sector, which matrix will not be used here. The lepton mixing matrix can then be written as the unitary matrix

$$U = R_{23} K R_{13} K^* R_{12} K' = \begin{pmatrix} c_{12} c_{13} & s_{12} c_{13} & s_{13} e^{-i\delta} \\ -s_{12} c_{23} - c_{12} s_{23} s_{13} e^{i\delta} & c_{12} c_{23} - s_{12} s_{23} s_{13} e^{i\delta} & s_{23} c_{13} \\ s_{12} s_{23} - c_{12} c_{23} s_{13} e^{i\delta} & -c_{12} s_{23} - s_{12} c_{23} s_{13} e^{i\delta} & c_{23} c_{13} \end{pmatrix} K' \quad (5)$$

where  $R_{ij}$  is the rotation matrix in the  $ij$  subspace,  $c_{ij} = \cos \theta_{ij}$ ,  $s_{ij} = \sin \theta_{ij}$ ,  $K = \text{diag}(e^{-i\delta}, 1, 1)$  and  $K'$  involves further possible phases due to Majorana mass terms that will contribute here.

In passing, we note that although this theoretical context is appealing, various modifications are possible. For example, string theory generically involves certain moduli fields which are singlets under the standard model gauge group, have flat superpotentials, and hence are massless in perturbation theory down to the energy scale where supersymmetry is broken. The spinor component fields, modulinos, can act as electroweak-singlet neutrinos, and may well have masses much less than the GUT scale (e.g. [43]). Moreover, models with a low string scale  $\ll M_{\text{Planck}}$  and large compact dimensions (e.g., [44]) also have implications for neutrino phenomenology. Here we shall work within the conventional seesaw-type scenario because of its simplicity and success in accounting for the most striking known feature of neutrinos, namely the fact that they are so light compared with the other known fermions.

For our later discussion it will be useful to record the formulas for the various relevant neutrino oscillation transitions. In the absence of any matter effect, the probability that a (relativistic) weak neutrino eigenstate  $\nu_a$  becomes  $\nu_b$  after propagating a distance  $L$  is

$$P(\nu_a \rightarrow \nu_b) = \delta_{ab} - 4 \sum_{i>j=1}^3 \text{Re}(K_{ab,ij}) \sin^2 \left( \frac{\Delta m_{ij}^2 L}{4E} \right) +$$

$$+ 4 \sum_{i>j=1}^3 \text{Im}(K_{ab,ij}) \sin\left(\frac{\Delta m_{ij}^2 L}{4E}\right) \cos\left(\frac{\Delta m_{ij}^2 L}{4E}\right) \quad (6)$$

where

$$K_{ab,ij} = U_{ai} U_{bi}^* U_{aj}^* U_{bj} \quad (7)$$

and

$$\Delta m_{ij}^2 = m(\nu_i)^2 - m(\nu_j)^2 \quad (8)$$

Recall that in vacuum, CPT invariance implies  $P(\bar{\nu}_b \rightarrow \bar{\nu}_a) = P(\nu_a \rightarrow \nu_b)$  and hence, for  $b = a$ ,  $P(\bar{\nu}_a \rightarrow \bar{\nu}_a) = P(\nu_a \rightarrow \nu_a)$ . For the CP-transformed reaction  $\bar{\nu}_a \rightarrow \bar{\nu}_b$  and the T-reversed reaction  $\nu_b \rightarrow \nu_a$ , the transition probabilities are given by the right-hand side of (6) with the sign of the imaginary term reversed. (Below we shall assume CPT invariance, so that CP violation is equivalent to T violation.) For most sets of parameters, only one mass scale is relevant for the neutrino oscillations of interest here, namely

$$\Delta m_{atm}^2 = \Delta m_{32}^2 \quad (9)$$

In this case, CP (T) violation effects are negligibly small, so that in vacuum

$$P(\bar{\nu}_a \rightarrow \bar{\nu}_b) = P(\nu_a \rightarrow \nu_b) \quad (10)$$

$$P(\nu_b \rightarrow \nu_a) = P(\nu_a \rightarrow \nu_b) \quad (11)$$

In the absence of T violation, the second equality (11) would still hold in matter, but even in the absence of CP violation, the first equality (10) would not hold. With the hierarchy (1), the expressions for the specific oscillation transitions are

$$\begin{aligned} P(\nu_\mu \rightarrow \nu_\tau) &= 4|U_{33}|^2 |U_{23}|^2 \sin^2\left(\frac{\Delta m_{atm}^2 L}{4E}\right) \\ &= \sin^2(2\theta_{23}) \cos^4(\theta_{13}) \sin^2\left(\frac{\Delta m_{atm}^2 L}{4E}\right) \end{aligned} \quad (12)$$

$$\begin{aligned} P(\nu_e \rightarrow \nu_\mu) &= 4|U_{13}|^2 |U_{23}|^2 \sin^2\left(\frac{\Delta m_{atm}^2 L}{4E}\right) \\ &= \sin^2(2\theta_{13}) \sin^2(\theta_{23}) \sin^2\left(\frac{\Delta m_{atm}^2 L}{4E}\right) \end{aligned} \quad (13)$$

$$\begin{aligned} P(\nu_e \rightarrow \nu_\tau) &= 4|U_{33}|^2 |U_{13}|^2 \sin^2\left(\frac{\Delta m_{atm}^2 L}{4E}\right) \\ &= \sin^2(2\theta_{13}) \cos^2(\theta_{23}) \sin^2\left(\frac{\Delta m_{atm}^2 L}{4E}\right) \end{aligned} \quad (14)$$

In neutrino oscillation searches using reactor antineutrinos, i.e. tests of  $\bar{\nu}_e \rightarrow \bar{\nu}_e$ , the two-species mixing hypothesis used to fit the data is

$$P(\nu_e \rightarrow \nu_e) = 1 - \sin^2(2\theta_{reactor}) \sin^2\left(\frac{\Delta m_{reactor}^2 L}{4E}\right) \quad (15)$$

where  $\Delta m_{reactor}^2$  is the squared mass difference relevant for  $\bar{\nu}_e \rightarrow \bar{\nu}_x$ . In particular, in the upper range of values of  $\Delta m_{atm}^2$ , since the transitions  $\bar{\nu}_e \rightarrow \bar{\nu}_\mu$  and  $\bar{\nu}_e \rightarrow \bar{\nu}_\tau$  contribute to  $\bar{\nu}_e$  disappearance, one has

$$P(\nu_e \rightarrow \nu_e) = 1 - \sin^2(2\theta_{13}) \sin^2\left(\frac{\Delta m_{atm}^2 L}{4E}\right) \quad (16)$$

i.e.,  $\theta_{reactor} = \theta_{13}$ , and the Chooz reactor experiment yields the bound [10]

$$\sin^2(2\theta_{13}) < 0.10 \quad (17)$$

which is also consistent with conclusions from the SuperK data analysis [6].

Further, the quantity “ $\sin^2(2\theta_{atm})$ ” often used to fit the data on atmospheric neutrinos with a simplified two-species mixing hypothesis, is, in the three-generation case,

$$\sin^2(2\theta_{atm}) \equiv \sin^2(2\theta_{23}) \cos^4(\theta_{13}) \quad (18)$$

Hence for small  $\theta_{13}$ , as implied by (17), it follows that, to good accuracy,  $\theta_{atm} = \theta_{23}$ .

### 3 Calculation of Matter Effects

The evolution of the flavor eigenstates of neutrinos is given by

$$i\frac{d}{dx}\nu = \left(\frac{1}{2E}UM^2U^\dagger + V\right)\nu \quad (19)$$

where

$$\nu = U\nu_m \quad (20)$$

$$\nu_m = \begin{pmatrix} \nu_1 \\ \nu_2 \\ \nu_3 \end{pmatrix} \quad (21)$$

$$M^2 = \begin{pmatrix} m_1^2 & 0 & 0 \\ 0 & m_2^2 & 0 \\ 0 & 0 & m_3^2 \end{pmatrix}, V = \begin{pmatrix} \sqrt{2}G_F N_e & 0 & 0 \\ 0 & 0 & 0 \\ 0 & 0 & 0 \end{pmatrix} \quad (22)$$

Here  $N_e$  is the electron number density and we have  $\sqrt{2}G_F N_e$  [eV] =  $7.6 \times 10^{-14} Y_e \rho$  [g/cm<sup>3</sup>].

The atmospheric neutrino data suggests almost maximal mixing in the 2 – 3 sector. However, a small but non-zero  $s_{13}$  is still allowed, and this produces the matter effect in the traversal of neutrinos through the Earth. We use the bound (17) on  $\sin^2(2\theta_{13})$  here, consistent with both the Chooz experiment [10] and the atmospheric neutrino data [6].

If we assume that the solar neutrino deficiency is explained by the small mixing angle (SMA) MSW solution or by vacuum oscillations, with the hierarchy of eq. (1), it follows that, for the relevant energies  $E \gtrsim 1$  GeV and path-lengths  $L \sim 10^3 - 10^4$  km, only one squared mass scale,  $\Delta m_{atm}^2$ , is important for the oscillations and the three-species neutrino oscillations can be described in terms of this quantity,  $\Delta m_{atm}^2$ , and the mixing parameters  $\sin^2(2\theta_{23})$ , and  $\sin^2(2\theta_{13})$ , with negligible dependence on  $\sin^2(2\theta_{12})$  and  $\delta$ .

In order to write down the probabilities of oscillation for long-baseline and atmospheric neutrinos, it is convenient to transform to a new basis defined by (e.g. [29])

$$\nu = R_{23}\tilde{\nu} \quad (23)$$

The evolution of  $\tilde{\nu}$  is given by

$$\tilde{H} = \frac{1}{2E}KR_{13}K^*R_{12}M^2R_{12}^\dagger KR_{13}^\dagger K^* + V \quad (24)$$

In the one mass-scale approximation, this can be reduced to

$$\tilde{H} \simeq \begin{pmatrix} \frac{1}{2E}s_{13}^2\Delta m_{32}^2 + \sqrt{2}G_F N_e & 0 & \frac{1}{2E}s_{13}c_{13}\Delta m_{32}^2 e^{-i\delta} \\ 0 & \frac{1}{2E}c_{12}^2\Delta m_{21}^2 & 0 \\ \frac{1}{2E}s_{13}c_{13}\Delta m_{32}^2 e^{i\delta} & 0 & \frac{1}{2E}c_{13}^2\Delta m_{32}^2 \end{pmatrix} \quad (25)$$

It can be seen now that in the basis  $(\nu_e, \tilde{\nu}_\mu, \tilde{\nu}_\tau)$  the three-flavor evolution equation decouples and it is enough to treat the two-flavor case. We define  $S$  and  $P$  by

$$\begin{pmatrix} \nu_e \\ \tilde{\nu}_\mu \\ \tilde{\nu}_\tau \end{pmatrix}(x) = S \begin{pmatrix} \nu_e \\ \tilde{\nu}_\mu \\ \tilde{\nu}_\tau \end{pmatrix}(0) \quad (26)$$

and

$$P \equiv |S_{13}|^2 = 1 - |S_{33}|^2 \quad (27)$$

Transforming back to the flavor basis  $(\nu_e, \nu_\mu, \nu_\tau)$ , the probabilities of oscillation become

$$P(\nu_e \rightarrow \nu_e) = 1 - P \quad (28)$$

$$P(\nu_e \rightarrow \nu_\mu) = P(\nu_\mu \rightarrow \nu_e) = s_{23}^2 P \quad (29)$$

$$P(\nu_e \rightarrow \nu_\tau) = c_{23}^2 P \quad (30)$$

$$P(\nu_\mu \rightarrow \nu_\mu) = 1 - s_{23}^4 P + 2s_{23}^2 c_{23}^2 [Re(S_{22}S_{33}) - 1] \quad (31)$$

$$P(\nu_\mu \rightarrow \nu_\tau) = s_{23}^2 c_{23}^2 [2 - P - 2Re(S_{22}S_{33})] \quad (32)$$

Note that for the mass hierarchy (1), the CP-violating phases disappear from the oscillation probabilities. In this case what we need to solve is the evolution equation for a two-flavor neutrino system. By subtracting from the diagonal the quantity  $\frac{1}{4E}\Delta m_{32}^2 + \frac{1}{\sqrt{2}}G_F N_e$ , this can be written in the form

$$i \frac{d}{dx} \begin{pmatrix} \nu_a \\ \nu_b \end{pmatrix} = \begin{pmatrix} -A(x) & B \\ B & A(x) \end{pmatrix} \begin{pmatrix} \nu_a \\ \nu_b \end{pmatrix} \quad (33)$$

with

$$A(x) = \frac{\Delta m_{32}^2}{4E} \cos(2\theta_{13}) - \frac{G_F}{\sqrt{2}} N_e(x) \quad (34)$$

$$B = \frac{\Delta m_{32}^2}{4E} \sin(2\theta_{13}) \quad (35)$$

For our purposes, we recall that the Earth is composed of crust, mantle, liquid outer core, and solid inner core, together with additional sublayers in the mantle, with particularly strong changes in density between the lower mantle and outer core. The density profile of the Earth is shown in Fig.1. The densities of the different layers are given in Table 1 as function of the normalized radius  $x = R/R_E$ ,  $R_E = 6371$  km being the radius of the Earth. The core has average density  $\rho_{core} = 11.83$  g/cm<sup>3</sup> and electron fraction  $Y_{e,core} = 0.466$ , while the mantle has average density  $\rho_{mantle} = 4.66$  g/cm<sup>3</sup> and  $Y_{e,mantle} = 0.494$ .

Radius [Km]	Density [g/cm <sup>3</sup> ]
0 – 1221.5	$13.0885 - 8.8381x^2$
1221.5 – 3480.0	$12.5815 - 1.2638x - 3.6426x^2 - 5.5281x^3$
3480.0 – 5701.0	$7.9565 - 6.4761x + 5.5283x^2 - 3.0807x^3$
5701.0 – 5771.0	$5.3197 - 1.4836x$
5771.0 – 5971.0	$11.2494 - 8.0298x$
5971.0 – 6151.0	$7.1089 - 3.8045x$
6151.0 – 6346.6	$2.6910 + 0.6924x$
6346.6 – 6356.0	2.900
6356.0 – 6371.0	2.600

**Table 1** Density Profile of the Earth

Since, to very good accuracy, the Earth is spherically symmetric (Fig.1), the neutrino flight path is described only by the zenith angle  $\theta_z$  (or  $\eta = \pi - \theta_z$ ). For

$$\frac{R_{i+1}}{R} < \sin \eta < \frac{R_i}{R} \quad (36)$$

the neutrinos pass through  $2i+1$  layers in the Earth. The distances traveled by the neutrinos in each of these layers are

$$L_1 = R \cos \eta - \sqrt{R_1^2 - R^2 \sin^2 \eta} \quad (37)$$

$$L_k = L_{2i+2-k} = \sqrt{R_{k-1}^2 - R^2 \sin^2 \eta} - \sqrt{R_k^2 - R^2 \sin^2 \eta}, \quad 2 \leq k \leq i \quad (38)$$

$$L_{i+1} = 2\sqrt{R_i^2 - R^2 \sin^2 \eta} \quad (39)$$

Studies have been done using the average density of the Earth along the neutrino path. In this case the evolution equation can be easily solved and the probability of oscillation is given by

$$P(\nu_a \rightarrow \nu_b) = \sin^2(2\theta_m) \sin^2(\omega L) \quad (40)$$

where  $\omega = \sqrt{A^2 + B^2}$  and  $\theta_m$  is the effective mixing in matter given by

$$\sin^2(2\theta_m) = \frac{\sin^2(2\theta)}{\sin^2(2\theta) + \left(\cos(2\theta) - \frac{2\sqrt{2}G_F N_e E}{\Delta m^2}\right)^2} \quad (41)$$

Just as was the case with the application of the MSW analysis to solar neutrinos, the key observation is that although the angle  $\theta$ , which is essentially  $\theta_{13}$  here, is small, the vanishing of the term in parentheses in the denominator of (41) renders the effective mixing angle  $\theta_m = \pi/4$ , thereby producing maximal mixing in matter. The important point is that, given the range of densities in the layers of the Earth, and the value of  $\Delta m_{atm}^2 \simeq 3.5 \times 10^{-3}$  eV<sup>2</sup>, this matter resonance occurs for neutrino energies of order  $O(10)$  GeV, in the range planned for long baseline neutrino oscillation experiments. Since this effect clearly depends on the sign of  $\Delta m^2$ , the measurement of matter effects can give information on this sign. When one takes account of the actual variable-density situation in the Earth, it is necessary to perform a numerical integration of the evolution equation, which we have done. We also go beyond the one mass-scale approximation and study the effect of  $\Delta m_{sol}^2$  and  $\theta_{12}$  on the oscillations. In this case we calculate the oscillation probabilities for nonzero values of all six oscillation parameters (three angles, one phase, and two mass square differences) and discuss when the simpler cases are very good approximations.

## 4 Results and Discussion

For long baseline experiments like K2K, MINOS, and CERN to Gran-Sasso, the neutrino flight path only goes through the upper mantle. The density in this region is practically constant, and the oscillation probabilities can easily be calculated. The matter effects are small, but possibly detectable for the longer baselines. We show in Fig.2 an example for  $P(\nu_\mu \rightarrow \nu_e)$  relevant for MINOS or the CERN to Gran-Sasso experiments (if SMA or VO solve the solar problem).

However, there are several motivations for very long baseline experiments, since, with sufficiently high-intensity sources, these can be sensitive to quite small values of  $\Delta m^2$  and since the matter effects, being larger, can amplify certain oscillations and can, in principle, be used to get information on the sign of  $\Delta m_{atm}^2$ . Hence we concentrate here on these very long baseline experiments; for these, the neutrino flight path goes through several layers of the Earth with different densities, including the lower mantle for some. We show results for the Fermilab to SLAC path length  $L \simeq 2900$  km and for  $L \simeq 7330$  km, the distance from Fermilab to Gran Sasso. Path lengths corresponding to the distance BNL to SLAC,  $L \simeq 4500$  km, and BNL to Gran Sasso,  $L \simeq 6560$  km, are also considered. We have also performed calculations for  $L \simeq 9200$  km, the Fermilab to SuperKamiokande path length.

In Fig.3 we compare the probabilities calculated with constant density along the neutrino path versus the results obtained by numerically integrating the evolution equation with the actual density profile of the Earth, as given by [41]. The results are almost the same for most of the parameter range. However, at given energies, as for example for the second maximum in  $P(\nu_\mu \rightarrow \nu_e)$ , the correction to the probability is of the order of 20%. The results in Fig.3

are obtained for the  $L = 7330$  km distance, for which the beam goes through all layers of the mantle. In [36] we gave a series of similar comparisons of oscillation probabilities calculated with the constant density approximation and with the actual density function. In the following, we only present results obtained with the actual density function in the Earth.

If one assumes the LMA solution to the solar neutrino problem, then for the  $L = 2900$  km baseline, both  $\Delta m_{atm}^2$  and  $\Delta m_{sol}^2$  have to be considered. In Fig.4 we show  $P(\nu_\mu \rightarrow \nu_e)$  and the  $\nu_\mu$  survival probability  $P(\nu_\mu \rightarrow \nu_\mu)$  as functions of energy for  $\Delta m_{atm}^2 = 3.5 \times 10^{-3}$  eV $^2$  and  $\sin^2 2\theta_{23} = 1$ , as suggested by the atmospheric data, and  $\sin^2 2\theta_{13} = 0.1$ , the maximum value allowed, and two different choices of  $\Delta m_{sol}^2$  and  $\sin^2 2\theta_{12}$ . One choice corresponds to the LMA solution, with  $\Delta m_{sol}^2 = 5 \times 10^{-5}$  eV $^2$  and  $\sin^2 2\theta_{12} = 0.8$ . For this LMA case, the choice of the CP violating phase  $\delta$  is relevant; here we take  $\delta = 0$  and compare with nonzero  $\delta$  below. The other choice is for the VO solution, with  $\Delta m_{sol}^2 = 10^{-10}$  eV $^2$  and  $\sin^2 2\theta_{12} = 1$ . The SMA solution gives the same results as the VO solution. One sees that the terms involving  $\Delta m_{sol}^2$  can have non-negligible effects on the  $\nu_\mu \rightarrow \nu_e$  oscillation probability for this path-length, especially at lower energies.

As noted earlier, in the one-mass scale approximation, there are no CP violation effects in these oscillations; however, when we take into account  $\Delta m_{sol}^2$ , we also have to consider CP-violating effects. We present in Fig.5 a comparison showing the results for the probabilities  $P(\nu_\mu \rightarrow \nu_e)$  and  $P(\nu_e \rightarrow \nu_\mu)$  for  $\delta = 0$  and  $\delta = \pi/2$ . We consider  $L = 2900$  km,  $\sin^2 2\theta_{23} = 1$ ,  $\sin^2 2\theta_{13} = 0.1$  and the LMA solution for the solar neutrino problem. We can see that the effects of the CP-violating phase are small. Note however that for non-zero CP-violation,  $P(\nu_\mu \rightarrow \nu_e) \neq P(\nu_e \rightarrow \nu_\mu)$ . For no CP-violation, even with matter effects, there is no difference between these two probabilities. Since with a muon storage ring, by switching between  $\mu^-$  and  $\mu^+$  beams, one could obtain both  $\nu_\mu$  and  $\nu_e$  beams, there is the possibility of searching for the CP (actually T) violating difference  $P(\nu_\mu \rightarrow \nu_e) - P(\nu_e \rightarrow \nu_\mu)$ . In practice, however, it would be difficult to identify the  $e^-$  from  $\nu_e$ , given that the  $\mu^-$  stored beam that yields the initial  $\nu_\mu$  also yields  $\bar{\nu}_e$ , which produce  $e^+$  in the detector, and given that it would be quite difficult to measure the sign of the  $e^\pm$  in planned detectors. An alternate method, to measure the asymmetry

$$D = \frac{P(\nu_e \rightarrow \nu_\mu) - P(\bar{\nu}_e \rightarrow \bar{\nu}_\mu)}{P(\nu_e \rightarrow \nu_\mu) + P(\bar{\nu}_e \rightarrow \bar{\nu}_\mu)} \quad (42)$$

is, in principle, possible, although it is complicated by the fact, as noted above, that  $D$  is rendered nonzero by matter effects even in the absence of CP violation (see also [37]). If the solar neutrino problem is solved by the SMA or vacuum oscillations, CP-violation effects are not observable in the experiments of interest here. Indeed, even for the LMA solution, the CP violation would be very hard to detect for path lengths larger than  $\sim 3000$  km because of matter effects.

For the Fermilab to Gran Sasso distance  $L \simeq 7330$  km (or the BNL to Gran Sasso distance  $L \simeq 6560$  km), the  $\Delta m_{sol}^2$  corrections are negligible, so we can analyze the problem using fewer relevant parameters:  $\Delta m_{atm}^2$ ,  $\theta_{13}$  and  $\theta_{23}$ . We calculate the oscillation probabilities in long baseline experiments as a function of  $E/\Delta m^2$ , rather than using a particular value for  $\Delta m^2$  or the energy. The relevant ranges are  $\Delta m^2 \sim \text{few} \times 10^{-3}$  eV $^2$  and energies  $E$

of the order of tens of GeV. This way of presenting the results can be useful in studying the optimization of the beam energy. We calculate the oscillation probabilities for different values of the mixing angles  $\theta_{13}$  and  $\theta_{23}$  allowed by the atmospheric neutrino data and the CHOOZ experiment.

We consider both neutrinos and antineutrinos. The matter effects reverse sign in these two cases; for antineutrinos,  $V$  in (22) is replaced with  $(-V)$ . This implies that if  $\Delta m^2$  is positive (as considered here), one can get a resonant enhancement of the oscillations for neutrinos, while for antineutrinos the matter effects would suppress the oscillations. The situation would be reversed if  $\Delta m^2$  were negative. The fact that the matter effects are opposite in sign for neutrinos and antineutrinos is well illustrated in Fig.2, where both results are presented, together with the vacuum case.

In order to study the effects at different distances, we show the same type of graphs for both  $L = 7330$  km and  $L = 2900$  km. For  $L = 2900$  km, the probabilities can be expressed as functions of  $E/\Delta m_{atm}^2$  only for the SMA and VO solutions to the solar neutrino problem. For LMA, small  $\Delta m_{sol}^2$  and CP violation corrections are added, as shown in Fig.4 and Fig.5.

We first study the survival probability of  $\nu_\mu$ . If the beam went through vacuum, the probability of oscillation would be given by Fig.6 for a wide range of allowed values of  $\sin^2(2\theta_{13})$ . In matter, this probability becomes sensitive to all oscillation parameters for longer baselines such as 7330 km. In order to illustrate this, we calculate the probability for  $\sin^2(2\theta_{13}) = 0.1$ , 0.04, and 0.01, and  $\sin^2(2\theta_{23}) = 0.8$  and  $\sin^2(2\theta_{23}) = 1$ . The results are presented in Fig.7 and Fig.8. Evidently, the matter effect increases as  $\theta_{13}$  increases (and vanishes if  $\theta_{13} = 0$ ). While the shift in the positions of the maxima and minima, as functions of  $E/\Delta m^2$  are small, there is a considerable change in the maximum at  $E/\Delta m^2 \simeq 3 \times 10^3$ . This is of great interest, since the use of a typical neutrino energy of  $E \sim 10$  GeV (somewhat less than the stored muon energy) would produce this value of  $E/\Delta m^2$ , given the central value  $\Delta m^2 = \Delta m_{atm}^2 \simeq 3.5 \times 10^{-3}$  eV<sup>2</sup> reported by SuperKamiokande [6].

We also want to compare the solution in vacuum (Fig.6), with the solution in matter for neutrinos (Figs. 7,8) and antineutrinos (Fig.9). For antineutrinos the  $\nu_\mu$  survival probability is not sensitive to the value of  $\theta_{13}$ . One can again see the opposite effects of matter on neutrinos and antineutrinos. The difference in the results for different mixing angles makes it possible, in principle, to use this probability for relatively precise measurements of the oscillation parameters. Measuring separately the probability for  $\nu_\mu$  and  $\bar{\nu}_\mu$  can be very useful in detecting the matter effects and using these to constrain the relevant mixings and squared mass difference. Clearly, if one could use two path lengths, as may be possible with a neutrino factory, this would provide more information and constraints.

The relative effects of matter can be especially dramatic in the oscillation probability  $P(\nu_e \rightarrow \nu_\mu)$ , since these directly involve  $\nu_e$ . Since the  $\nu_e$  beam would arise from a stored  $\mu^+$  beam, and the  $\bar{\nu}_\mu$ 's from the decays of the  $\mu^+$ 's would produce  $\mu^+$ 's in the detector, the signature for the  $\nu_e \rightarrow \nu_\mu$  oscillation would be wrong-sign muons. As noted above, planned detectors would be capable of searching for such wrong-sign muons. Since this is a sub-dominant channel, the oscillation effect is small. If the beam went through the vacuum,  $P(\nu_e \rightarrow \nu_\mu)$  would probably be too small to detect, as is evident in Fig.10 (This shows  $P(\nu_\mu \rightarrow \nu_e)$ , which is equal to  $P(\nu_e \rightarrow \nu_\mu)$  for the present situation where CP violation is

negligible.) Because of the matter effect however, this probability can be strongly enhanced, as is evident in Fig.11 and Fig.12. For  $L = 7330$  km, the enhancement is largest for  $E/\Delta m^2 \simeq 2.5 \times 10^3$  GeV/eV<sup>2</sup>. This is close to the ratio that one would get for a neutrino energy of  $E \sim 10$  GeV, given the indication from the data that  $\Delta m_{atm}^2 = 3.5 \times 10^{-3}$  eV<sup>2</sup>. For  $L = 2900$  km, the largest enhancement is obtained for  $E/\Delta m^2$  a factor of 3 lower. We also show in this case the results for the baselines corresponding to possible BNL-SLAC and BNL-Gran Sasso distances; see Fig.13. As is evident, the matter effect can amplify  $P(\nu_e \rightarrow \nu_\mu)$  and enable this transition to be measured with good accuracy, thereby yielding very important information on the oscillation parameters. This probability is quite sensitive to the value of  $\theta_{13}$ , so one should be able to use it for a good determination of this angle. This physics capability motivates careful design studies to optimize the choice of  $L$  and  $E$  for this measurement. The sensitivity to  $\Delta m^2$  is also quite strong, due to the pronounced peak given by the matter effect in the relevant region. Note that for antineutrinos, the oscillation is suppressed (Fig.14), so an independent measurement of the two channels ( $\nu_\mu \rightarrow \nu_e$  and  $\bar{\nu}_\mu \rightarrow \bar{\nu}_e$ ) would be very valuable.

The atmospheric neutrino data tells us that the dominant oscillation channel is actually  $\nu_\mu \rightarrow \nu_\tau$ . Consequently, it would be very useful to measure  $P(\nu_\mu \rightarrow \nu_\tau)$ ; this would provide further confirmation of this oscillation and could also provide further information on  $\Delta m^2$  and  $\theta_{23}$ . In addition to the MINOS experiment [14], the ICANOE and OPERA detectors that will operate in the CERN to Gran Sasso neutrino beam envision  $\tau$  appearance capabilities [21, 22]. Results for  $P(\nu_\mu \rightarrow \nu_\tau)$  are presented in Fig.15, and Fig.16 shows  $P(\bar{\nu}_\mu \rightarrow \bar{\nu}_\tau)$ . Next, we present  $P(\nu_e \rightarrow \nu_\tau)$  in Fig.17 and  $P(\bar{\nu}_e \rightarrow \bar{\nu}_\tau)$  in Fig.17. These calculations show that matter effects are important and enhance oscillations of the neutrinos and suppress oscillations of antineutrinos in the relevant region of parameters. By combining results from different types of measurements, in different channels of oscillations, the allowed parameter space can be strongly constrained, leading to precise measurements of all mixings and  $\Delta m^2$ .

For a baseline over 9000 km, as would be the case for an experiment from Fermilab to SuperKamiokande, the main features discussed above remain true. Matter effects are significant for the oscillation of neutrinos for  $\Delta m^2$  in the region suggested by the atmospheric data and energies of the order of 10 GeV. Due to the matter effects, oscillation probabilities become very sensitive to  $\theta_{13}$ . Matter effects also improve the sensitivity to  $\Delta m^2$ . Since matter effects for antineutrinos are opposite to those for neutrinos, independent measurements of neutrino and antineutrino oscillations would give a precise measure of the matter effects and, consequently, of the parameters relevant to the oscillations. Due to the longer path through the Earth with bigger density, the matter effects can become even more dramatic. However, the statistics of the experiment would be limited by the lower neutrino flux at larger distances, and a careful study is necessary in order to choose optimal values of  $L$  and  $E$ .

## 5 Summary

To summarize, in planning for very long baseline neutrino oscillation experiments, it is important to take into account matter effects. These effects are significant for the range of

neutrino energies  $E$  of order 10's of GeV that are planned for these experiments, given the density of the Earth and the value of  $\Delta m_{atm}^2 \sim 3 \times 10^{-3}$  eV $^2$  indicated by current atmospheric neutrino data. We have performed a study of these including realistic density profiles in the earth. Matter effects can be useful in amplifying neutrino oscillation signals and helping one to obtain measurements of mixing parameters and the magnitude and sign of  $\Delta m_{atm}^2$ .

### Acknowledgments

We thank Bob Bernstein and Debbie Harris for helpful comments and have benefitted from participation in the ongoing working groups studying the design and physics capabilities of storage rings as neutrino factories [17, 20]. The research of R. S. was supported in part at Stony Brook by the U. S. NSF grant PHY-97-22101 and at Brookhaven by the U.S. DOE contract DE-AC02-98CH10886.<sup>3</sup>

## References

- [1] Fits and references to the Homestake, Kamiokande, GALLEX, SAGE, and Super Kamiokande data include N. Hata and P. Langacker, Phys. Rev. **D56**, 6107 (1997); J. Bahcall, P. Krastev, A. Smirnov, Phys. Rev. **D58**, 096016 (1998); J. Bahcall and P. Krastev, Phys. Lett. **B436**, 243 (1998) and <http://www.sns.ias.edu/~jnb/>. Recent Super Kamiokande data is reported in Super Kamiokande Collab., Y. Fukuda et al., Phys. Rev. Lett. **82**, 1810, 243 (1999).
- [2] L. Wolfenstein, Phys. Rev. **D17**, 2369 (1978).
- [3] S. P. Mikheyev and A. Smirnov, Yad. Fiz. **42**, 1441 (1985) [Sov.J. Nucl. Phys. **42**, 913 (1986)], Nuovo Cim., **C9**, 17 (1986).
- [4] Kamiokande Collab., K. S. Hirata, Phys. Lett. **B205**, 416; *ibid.* **280**, 146 (1992); Y. Fukuda et al., Phys. Lett. **B335**, 237 (1994); S. Hatakeyama et al. Phys. Rev. Lett. **81**, 2016 (1998).
- [5] IMB Collab., D. Casper et al., Phys. Rev. Lett. **66**, 2561 (1991); R. Becker-Szendy et al., Phys. Rev. **D46**, 3720 (1992); Phys. Rev. Lett. **69**, 1010 (1992).
- [6] Super-Kamiokande Collab., Y. Fukuda et al., Phys. Lett. **B433**, 9 (1998); Phys. Rev. Lett. **81**, 1562 (1998); *ibid.*, **82**, 2644 (1999); Phys. Lett. **B467**, 185 (1999).
- [7] Soudan Collab., W. Allison et al, Phys. Lett. **B391**, 491 (1997); Soudan-2 Collab., Phys. Lett. **B449**, 137 (1999); A. Mann, in Proceedings of the 1999 Photon-Lepton Symposium, hep-ex/9912007.
- [8] MACRO Collab., M. Ambrosio et al., Phys. Lett. **B434**, 451 (1998); hep-ex/0001044.

---

<sup>3</sup>Accordingly, the U.S. government retains a non-exclusive royalty-free license to publish or reproduce the published form of this contribution or to allow others to do so for U.S. government purposes.

- [9] J. Learned, in the Proceedings of the Workshop on the Next Generation Nucleon Decay and Neutrino Detector NNN99, Stony Brook (Sept. 1999).
- [10] M. Apollonio et al., Phys. Lett. **B420**, 397 (1998); Phys. Lett. **B466**, 415 (1999).
- [11] For recent experimental reviews, see, e.g., L. DiLella, hep-ex/9912010; H. Robertson, hep-ex/0001034, and talks at the Workshop on the Next Generation Nucleon Decay and Neutrino Detector NNN99, Stony Brook (Sept. 1999),  
[http://superk.physics.sunysb.edu/NNN99/scientific\\_program/](http://superk.physics.sunysb.edu/NNN99/scientific_program/). A large number of references to theory papers may be found in the review S. M. Bilenky, C. Giunti, and W. Grimus, hep-ph/9812360.
- [12] LSND Collab., C. Athanassopoulous et al., Phys. Rev. Lett. **77**, 3082 (1996), LSND Collab., C. Athanassopoulous et al., Phys. Rev. Lett. **81**, 1774 (1998).
- [13] KARMEN Collab., K. Eitel, B. Zeitnitz, in Proceedings of Neutrino-98, Nucl. Phys. (Proc. Suppl.) **77**, 212 (1999).
- [14] References and websites for these experiments and future projects can be found, e.g., at [http://www.hep.anl.gov/ndk/hypertext/nu\\_industry.html](http://www.hep.anl.gov/ndk/hypertext/nu_industry.html).
- [15] S. Geer, Phys. Rev. **D57**, 6989 (1998).
- [16] De Rujula, M. B. Gavela, and P. Hernandez, Nucl. Phys. **B547**, 21 (1999).
- [17] Some relevant websites at BNL, FNAL, and CERN containing further information are  
<http://www.cap.bnl.gov/mumu/> [http://www.fnal.gov/projects/muon\\_collider/physics/](http://www.fnal.gov/projects/muon_collider/physics/)  
<http://www.cern.ch/~autin/nufact99/whitepap.ps>
- [18] Workshop on the Potential for Neutrino Physics at Future Muon Colliders, BNL (Aug. 1998), <http://pubweb.bnl.gov/people/bking/nushop/workshop.html>.
- [19] Neutrino Factory and Muon Collider Collaboration, Expression of Interest for R+D towards a Neutrino Factory Based on a Storage Ring and Muon Collider, physics/9911009, <http://puhep1.princeton.edu/mumu/NSFLetter/nsfmain.ps>. This site also contains further references to the relevant literature.
- [20] I. Bigi et al., The Potential for Neutrino Physics at Muon Colliders and Other High-Current Muon Storage Rings, to appear in Phys. Rept.; see also  
<http://pubweb.bnl.gov/people/bking/nushop>.
- [21] ICANOE Collab. F. Cavanna et al., LNGS-P21-99-ADD-1,2, Nov 1999; A. Rubbia, hep-ex/0001052.
- [22] OPERA Collab., CERN-SPSC-97-24, hep-ex/9812015.

[23] V. Barger, K. Whisnant, S. Pakvasa, and R. J. N. Phillips, Phys. Rev. **D22**, 2718 (1980). See also V. Barger, K. Whisnant, and R. J. N. Phillips, Rev. Rev. Lett. **45**, 2084 (1980).

[24] D. Ayres, T. Gaisser, A. K. Mann, and R. Shrock, in *Proceedings of the 1982 DPF Summer Study on Elementary Particles and Future Facilities*, Snowmass, p. 590; D. Ayres, B. Cortez, T. Gaisser, A. K. Mann, R. Shrock, and L. Sulak, Phys. Rev. **D29**, 902 (1984).

[25] P. Krastev, S. Petcov, Phys. Lett. **B205**, 8 (1988).

[26] A. J. Baltz, J. Weneser, Phys. Rev. **D37**, 3364 (1988).

[27] C. W. Kim and A. Pevsner, *Neutrinos in Physics and Astrophysics* (Harwood, Langhorne, 1993).

[28] S. Petcov, Phys. Lett. **B434**, 321 (1998). M. Chizhov, M. Maris, S. Petcov, hep-ph/9810501; M. Chizhov, S. Petcov, hep-ph/9903424; M. Chizhov, S. Petcov, Phys. Rev. Lett. **83**, 1096 (1999).

[29] E. Akhmedov, A. Dighe, P. Lipari, A. Smirnov, Nucl. Phys. **B542**, 3 (1999); E. Akhmedov, Nucl. Phys. **B538**, 25 (1999); hep-ph/0001264.

[30] R. H. Bernstein and S. J. Parke, Phys. Rev. **D44**, 2069 (1991).

[31] P. Lipari, hep-ph/9903481.

[32] M. Campanelli, A. Bueno, A. Rubbia, hep-ph/9905240.

[33] S. Dutta, R. Gandhi, and B. Mukhopadhyaya, hep-ph/9905475.

[34] V. Barger, S. Geer, K. Whisnant, Phys. Rev. **D61**, 053004 (2000).

[35] D. Dooling, C. Giunti, K. Kang, C. W. Kim, hep-ph/9908513.

[36] I. Mocioiu, R. Shrock, in the Proceedings of the Workshop on the Next Generation Nucleon Decay and Neutrino Detector NNN99, Stony Brook (Sept. 1999), hep-ph/9910554.

[37] S.M. Bilenky, C. Giunti, W. Grimus, Phys. Rev. **D58**, 033001 (1998); K. Dick, M. Freund, M. Lindner, A. Romanino, Nucl. Phys. **B562**, 29 (1999); M. Tanimoto, Phys. Lett. **B462**, 115 (1999); A. Donini, M.B. Gavela, P. Hernandez, S. Rigolin, hep-ph/9909254; M. Koike, J. Sato, hep-ph/9909469; P.F. Harrison, W.G. Scott, hep-ph/9912435.

[38] V. Barger, S. Geer, R. Raja, K. Whisnant, hep-ph/9911524.

[39] M. Freund, T. Ohlsson, hep-ph/9909501; T. Ohlsson, H. Snellman, hep-ph/9910546, hep-ph/9912295.

[40] M. Freund, M. Lindner, S.T. Petcov, A. Romanino, hep-ph/9912457.

- [41] A.Dziewonski, Earth Structure, in: "The Encyclopedia of Solid Earth Geophysics", D.E.James (Ed.), (Van Nostrand Reinhold, New York, 1989), p.331.
- [42] M. Gell-Mann, P. Ramond, R. Slansky, in *Supergravity*, edited by P. van Nieuwenhuizen and D. Freedman (North Holland, Amsterdam, 1979), p. 315; T. Yanagida in proceedings of *Workshop on Unified Theory and Baryon Number in the Universe*, KEK, 1979.
- [43] K. Benakli and A. Smirnov, Phys. Rev. Lett. **79**, 4314 (1997).
- [44] N. Arkani-Hamed, S. Dimopoulos, and G. Dvali, Phys. Rev. **D59**, 086004 (1999); N. Arkani-Hamed, S. Dimopoulos, G. Dvali, and J. March-Russell, hep-ph/9811448 and references therein.

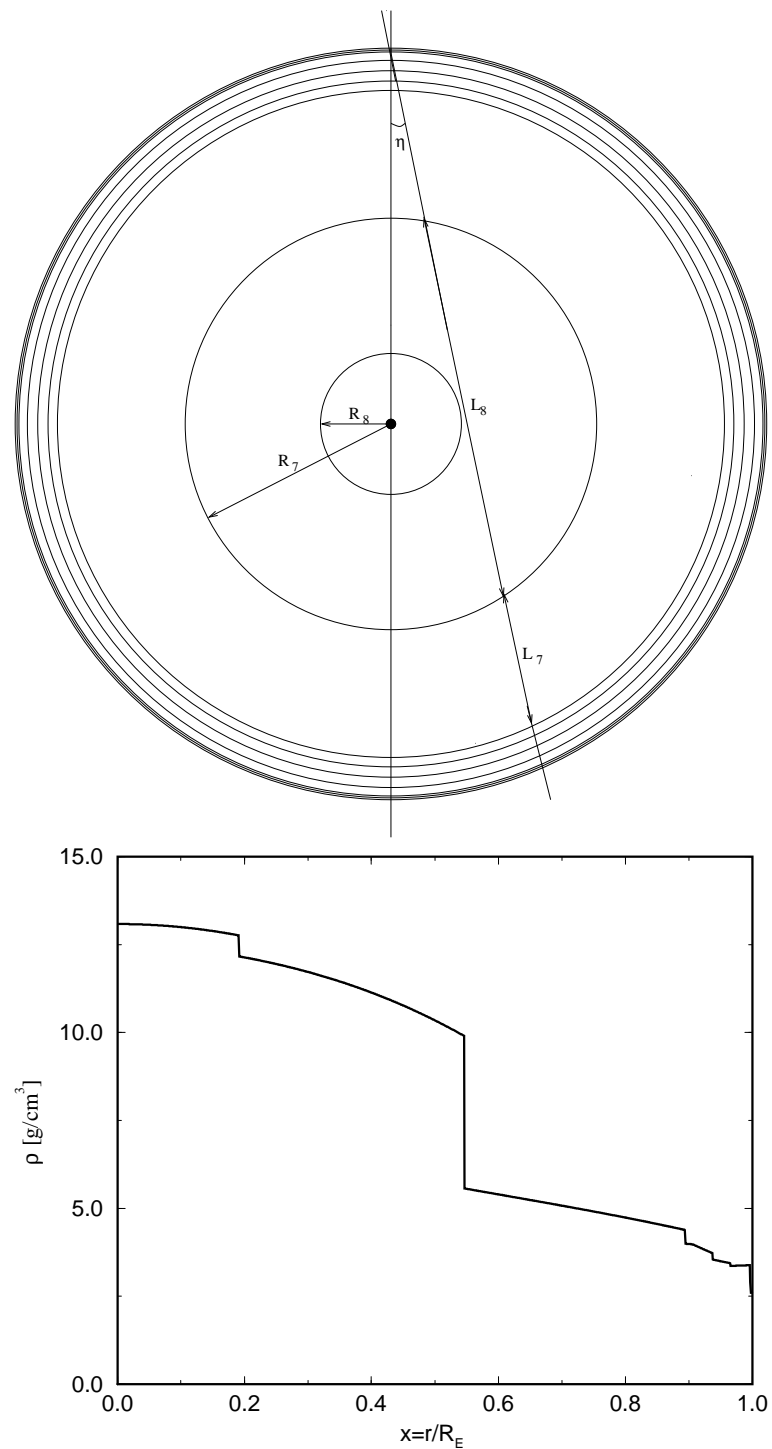


Figure 1: Density profile of the Earth.

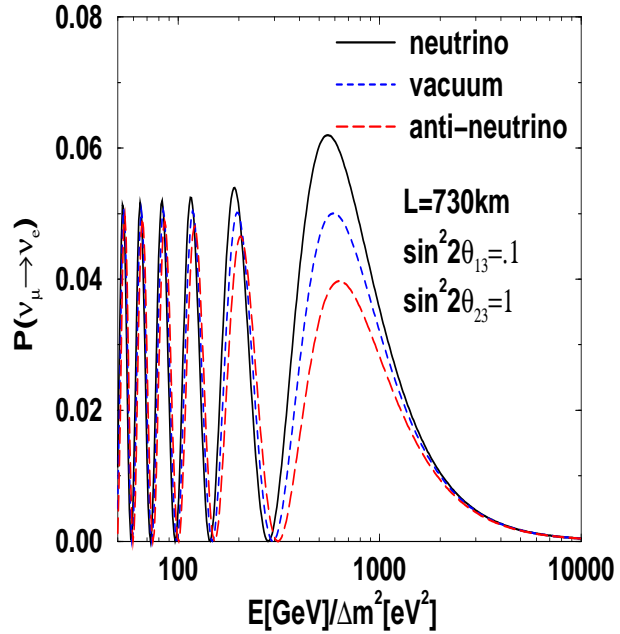


Figure 2:  $P(\nu_\mu \rightarrow \nu_e)$  and  $P(\bar{\nu}_\mu \rightarrow \bar{\nu}_e)$  in matter and in vacuum for  $L = 730$  km. (Figure legend is understood to include both cases.) Here  $\sin^2(2\theta_{13}) = 0.1$  and  $\sin^2(2\theta_{23}) = 1$ .

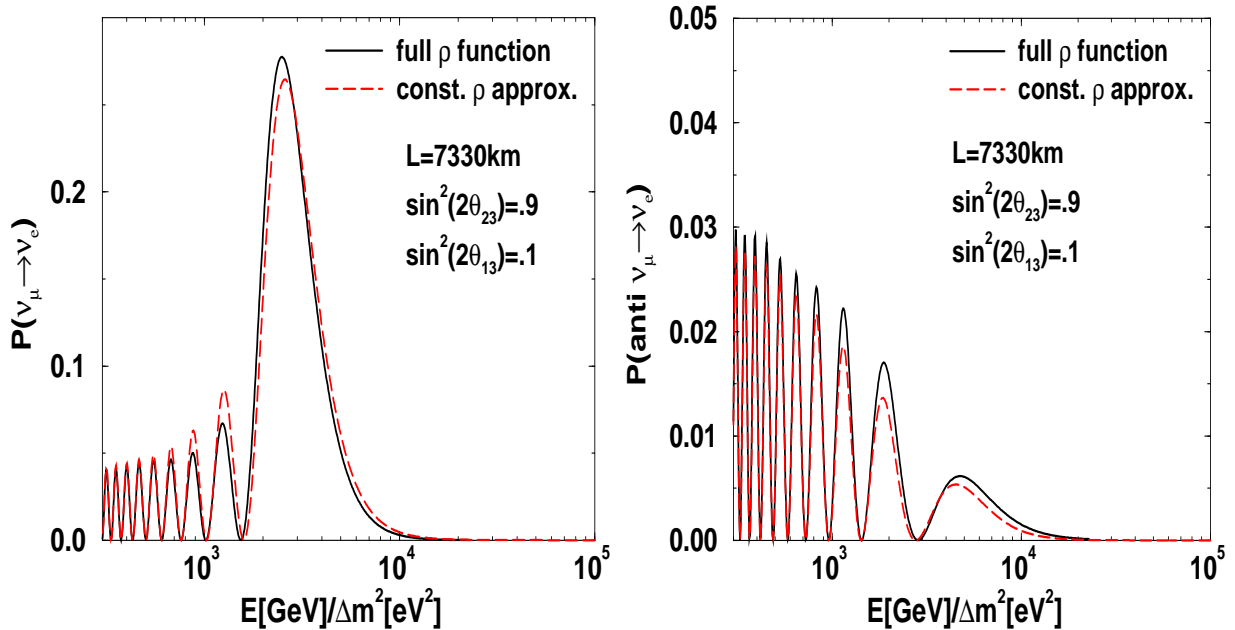


Figure 3:  $P(\nu_\mu \rightarrow \nu_e)$  and  $P(\bar{\nu}_\mu \rightarrow \bar{\nu}_e)$  with density function given by the full model of the Earth, compared with constant density approximation, for  $L = 7330$  km with  $\sin^2(2\theta_{13}) = 0.1$  and  $\sin^2(2\theta_{23}) = 0.9$ .

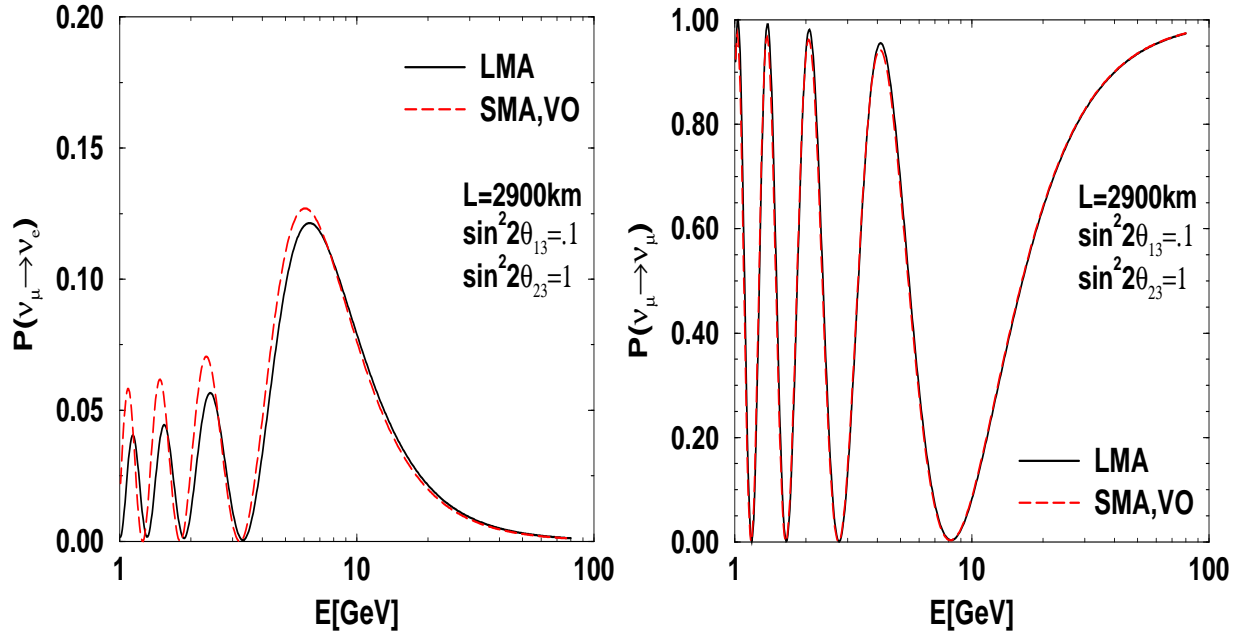


Figure 4:  $P(\nu_\mu \rightarrow \nu_e)$  and  $P(\nu_\mu \rightarrow \nu_\mu)$  for various solutions to the solar neutrino problem. Here  $L = 2900$  km,  $\sin^2(2\theta_{13}) = 0.1$ ,  $\sin^2(2\theta_{23}) = 1$ , and  $\Delta m_{atm}^2 = 3.5 \times 10^{-3}\text{eV}^2$ .

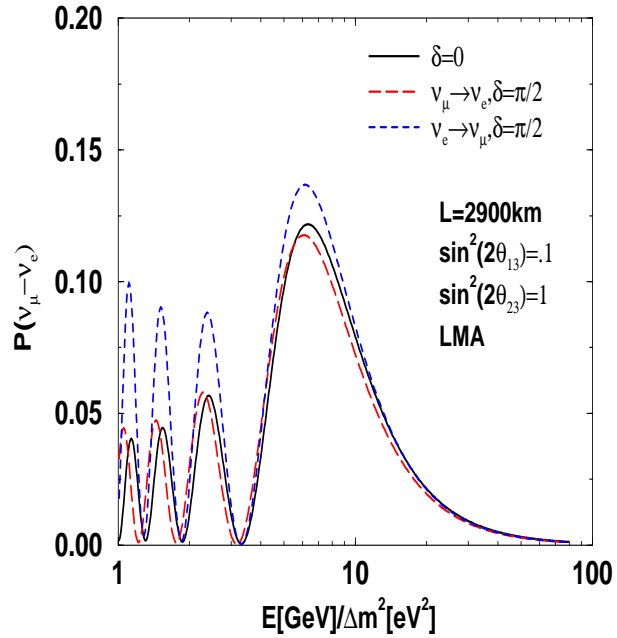


Figure 5: CP-violation effects for  $L = 2900$  km,  $\sin^2(2\theta_{23}) = 1$ ,  $\sin^2(2\theta_{13}) = 0.1$ , LMA solution,  $\delta = 0, \pi/2$ .

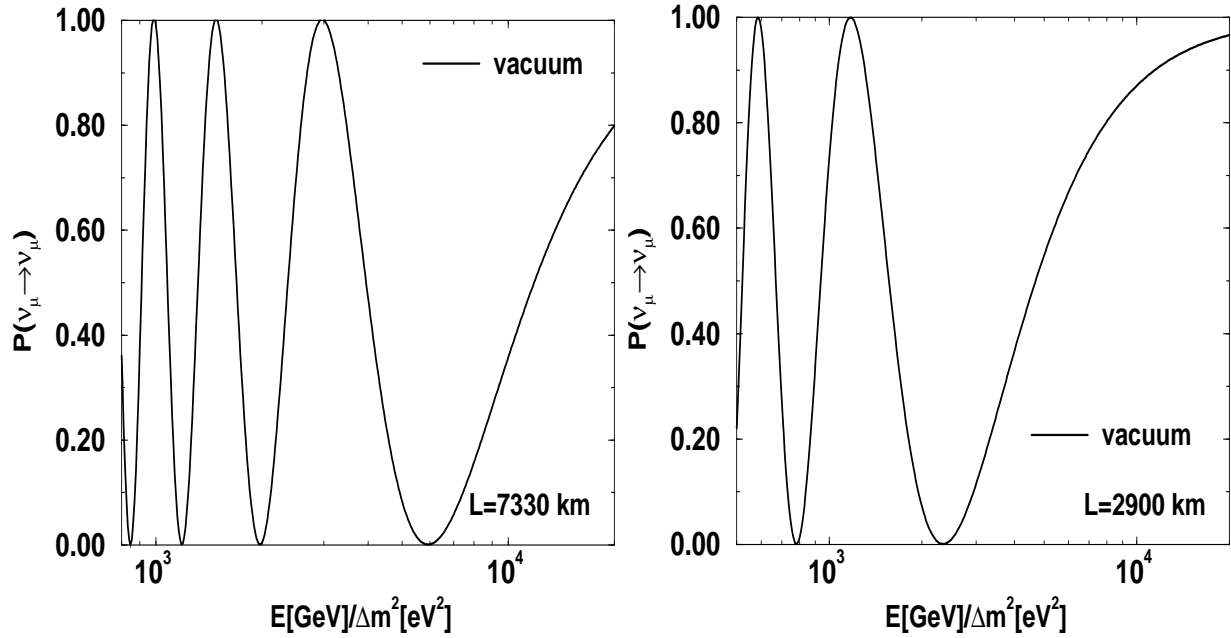


Figure 6: Hypothetical plot of  $P(\nu_\mu \rightarrow \nu_\mu)$  in vacuum for  $L = 7330$  km,  $L = 2900$  km with  $\sin^2(2\theta_{23}) = 1$ , for comparison with other plots incorporating matter effects.

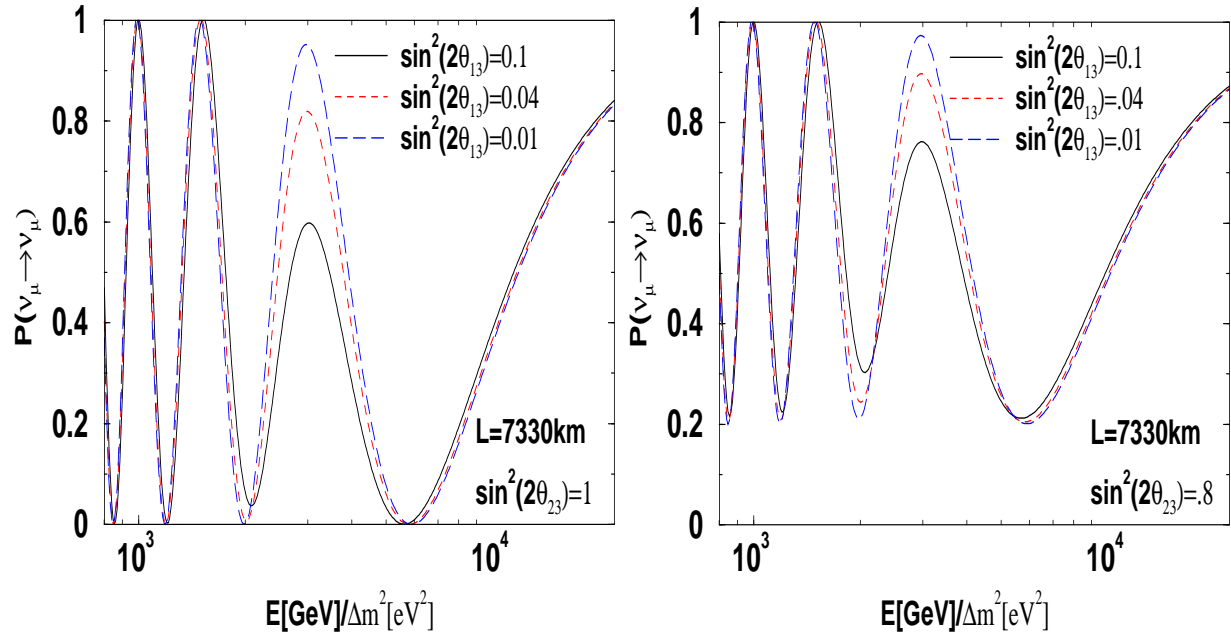


Figure 7:  $P(\nu_\mu \rightarrow \nu_\mu)$  for  $L = 7330$  km with  $\sin^2(2\theta_{13}) = 0.1, .04, .01$  and  $\sin^2(2\theta_{23}) = 1, 0.8$ .

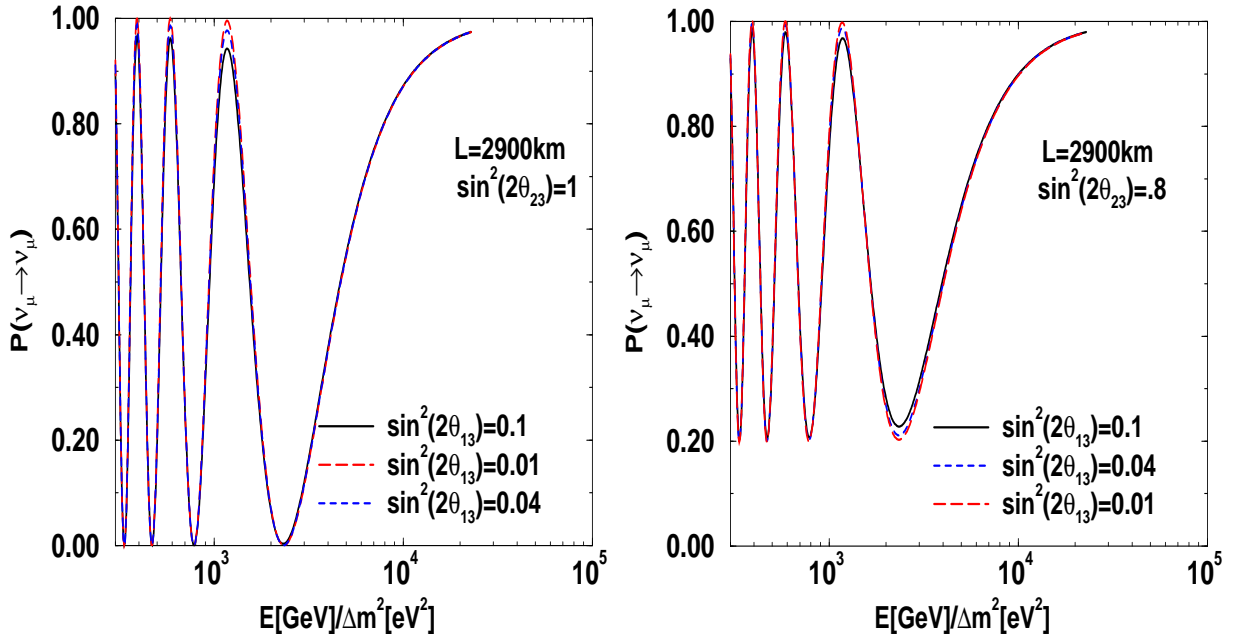


Figure 8: Same as Fig. 7 for  $L = 2900$  km.

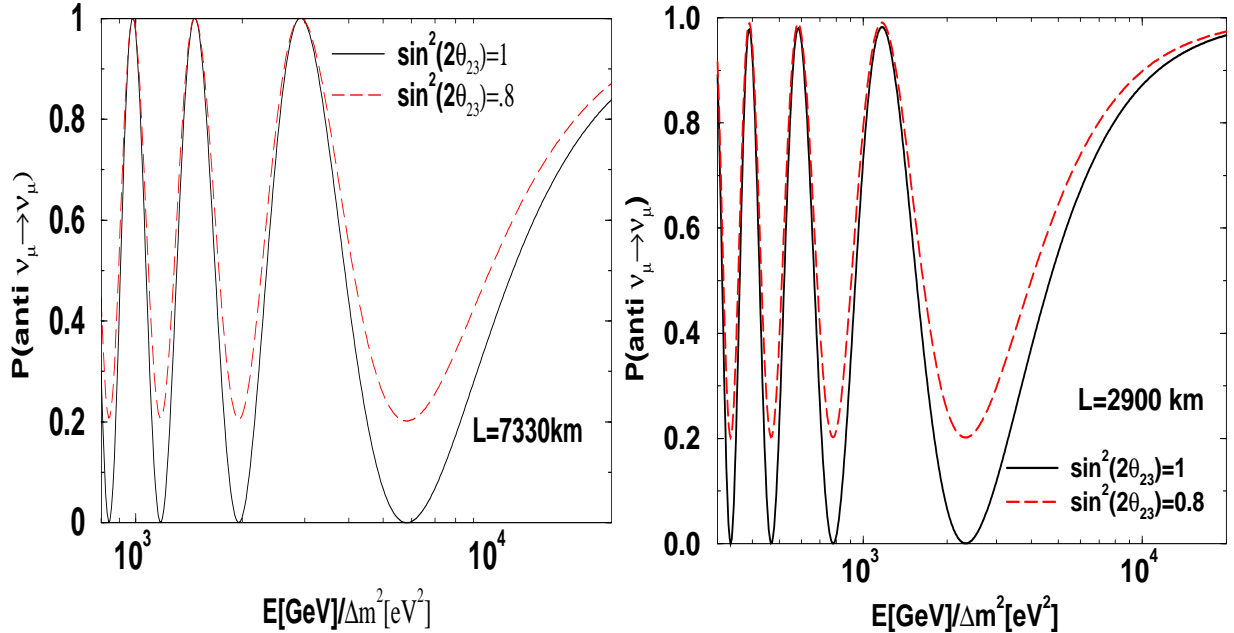


Figure 9:  $P(\bar{\nu}_\mu \rightarrow \bar{\nu}_\mu)$  for  $L = 7300$  km,  $L = 2900$  km with  $\sin^2(2\theta_{23}) = 1, 0.8$  and  $\sin^2(2\theta_{13}) = 0.1$ .

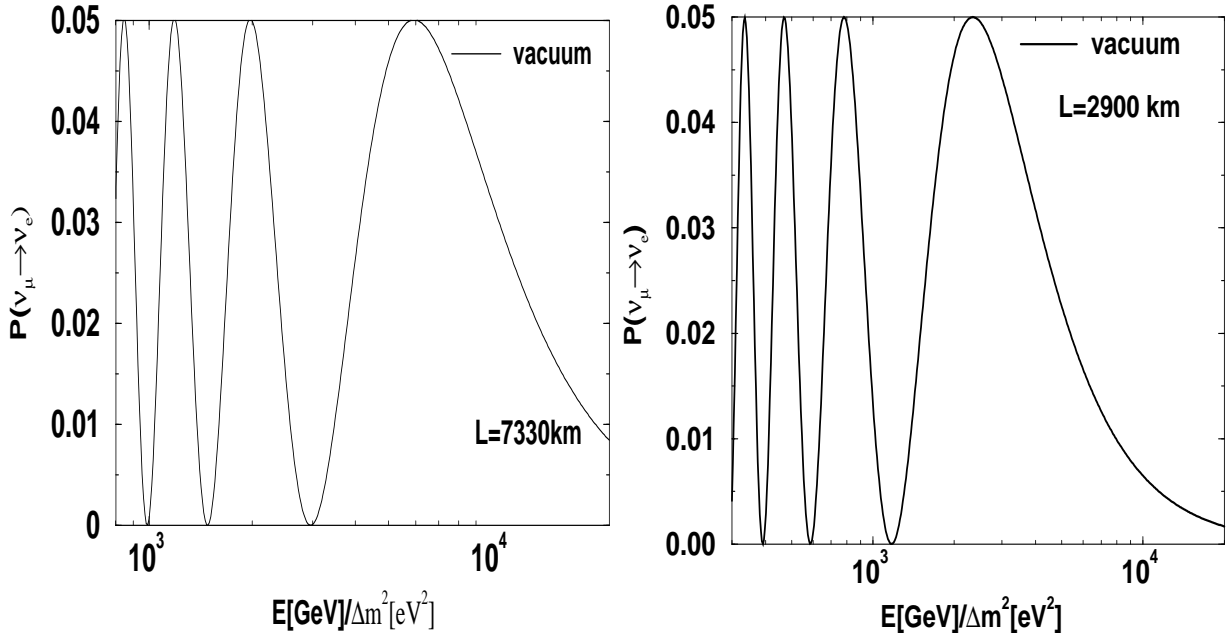


Figure 10: Hypothetical  $P(\nu_\mu \rightarrow \nu_e)$  in vacuum for  $L = 7330$  km and  $L = 2900$  km with  $\sin^2(2\theta_{13}) = 0.1$  and  $\sin^2(2\theta_{23}) = 1$  for comparison with other plots incorporating matter effects.

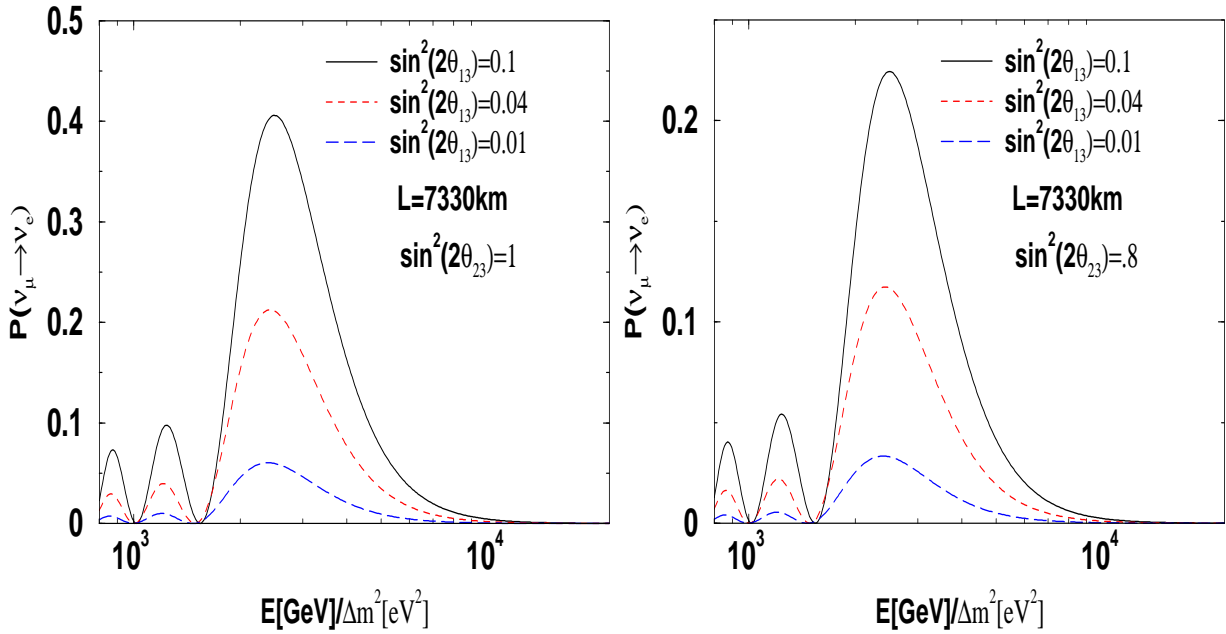


Figure 11:  $P(\nu_\mu \rightarrow \nu_e)$  for  $L = 7300$  km with  $\sin^2(2\theta_{13}) = 0.1, 0.04, 0.01$  and  $\sin^2(2\theta_{23}) = 1, 0.8$ .

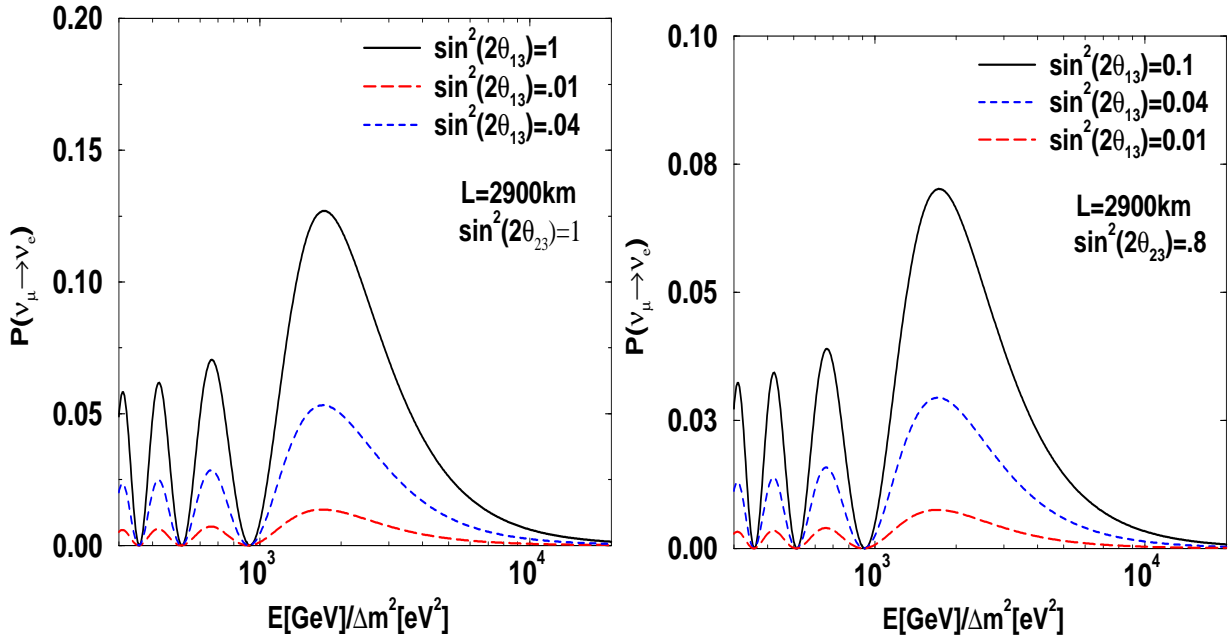


Figure 12: Same as Fig. 11 for  $L = 2900$  km.

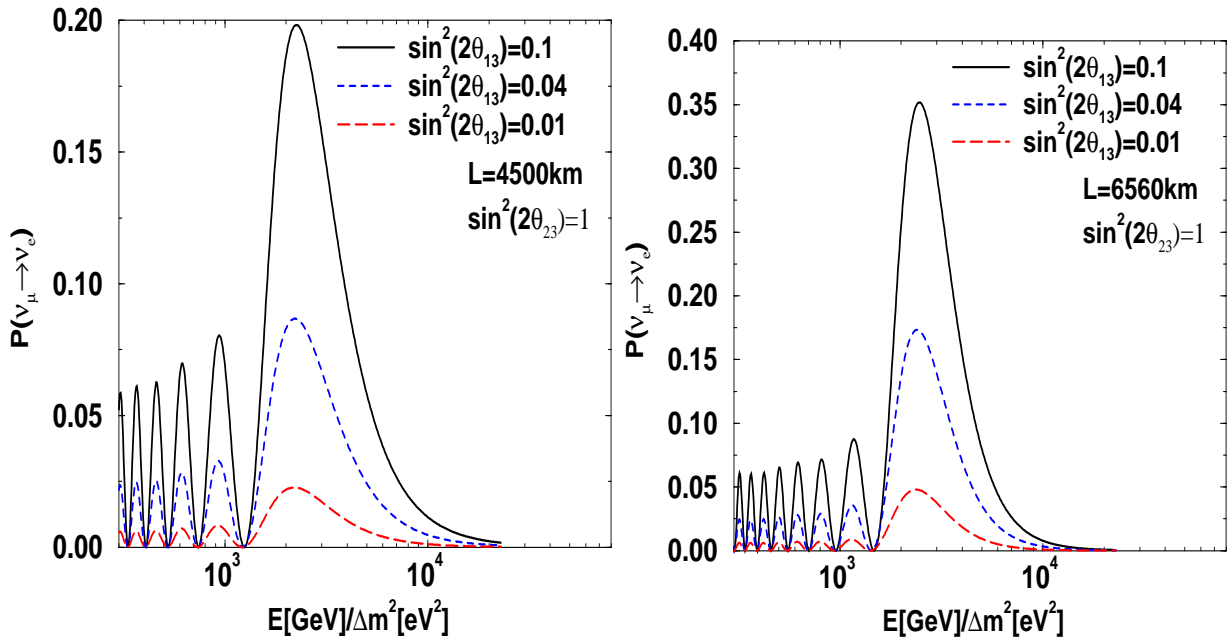


Figure 13:  $P(\nu_\mu \rightarrow \nu_e)$  for  $L = 4500$  km,  $L = 6560$  with  $\sin^2(2\theta_{13}) = 0.1, 0.04, 0.01$  and  $\sin^2(2\theta_{23}) = 1$ .

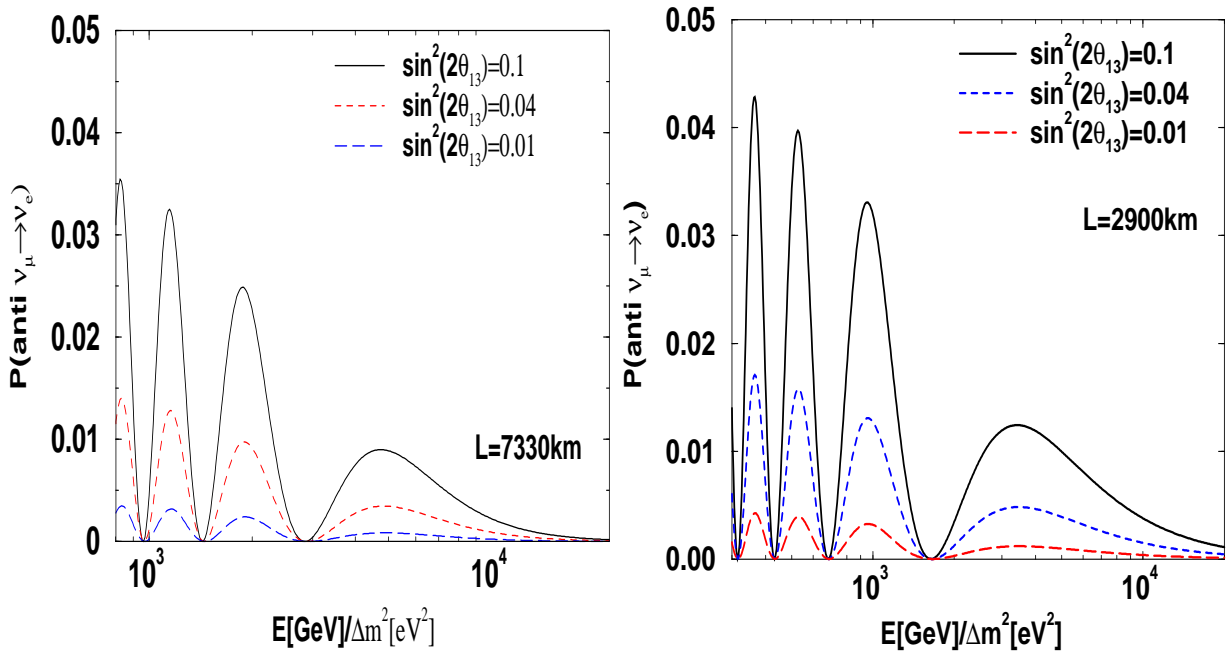


Figure 14:  $P(\bar{\nu}_\mu \rightarrow \bar{\nu}_e)$  for  $L = 7300$  km and  $L = 2900$  km with  $\sin^2(2\theta_{13}) = 0.1, .04, .01$  and  $\sin^2(2\theta_{23}) = 1$ .

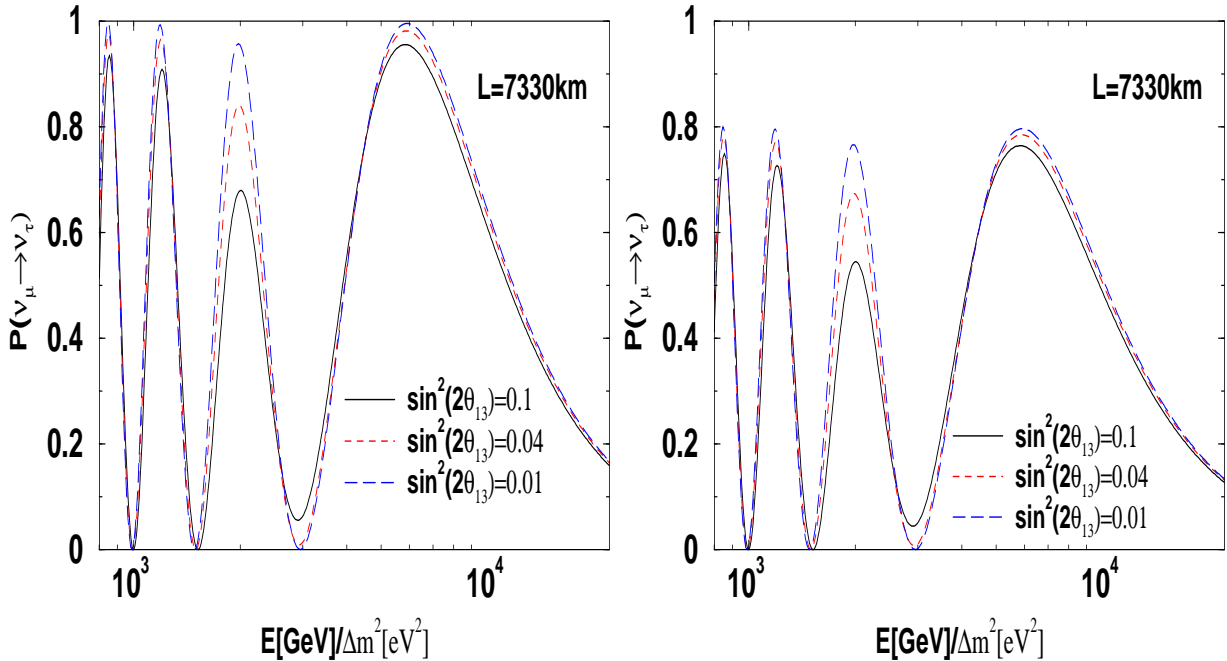


Figure 15:  $P(\nu_\mu \rightarrow \nu_\tau)$  for  $L = 7330$  km with  $\sin^2(2\theta_{13}) = 0.1, 0.04, 0.01$  and  $\sin^2(2\theta_{23}) = 1$ .

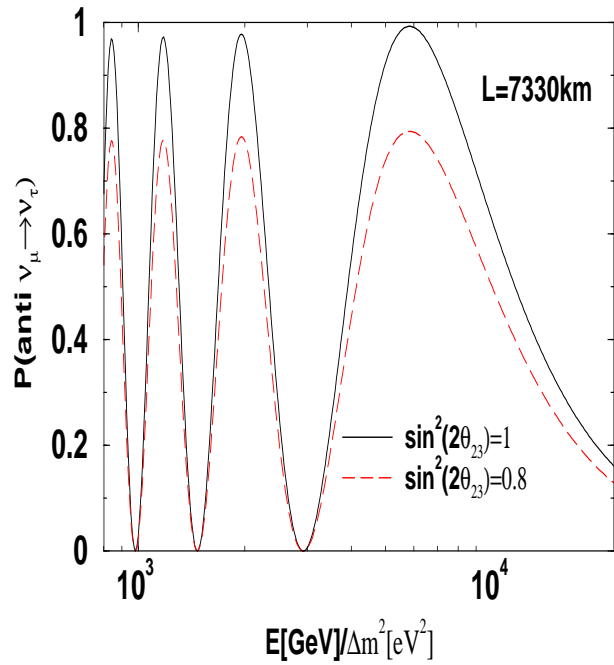


Figure 16:  $P(\bar{\nu}_\mu \rightarrow \bar{\nu}_\tau)$  for  $L = 7330$  km with  $\sin^2(2\theta_{13}) = 0.1$  and  $\sin^2(2\theta_{23}) = 1, 0.8$ .

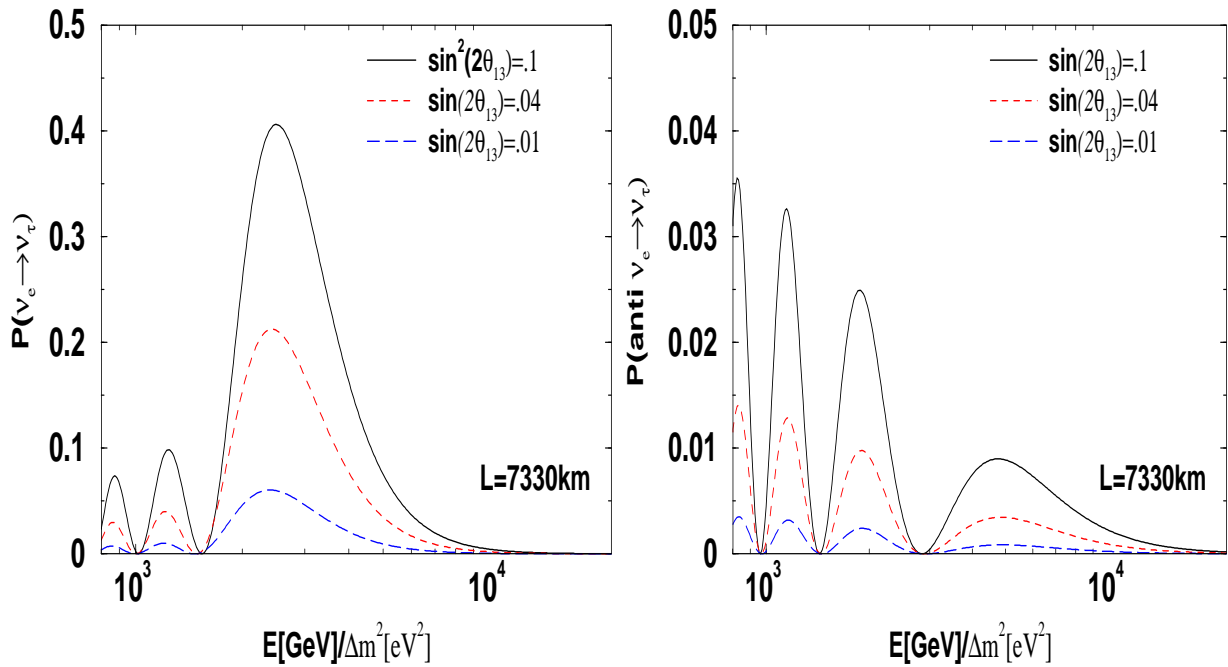


Figure 17:  $P(\nu_e \rightarrow \nu_\tau)$  and  $P(\bar{\nu}_e \rightarrow \bar{\nu}_\tau)$  for  $L = 7330$  with  $\sin^2(2\theta_{13}) = 0.1, 0.04, 0.01$  and  $\sin^2(2\theta_{23}) = 1$ .